Supplement of Atmos. Chem. Phys., 21, 457–481, 2021
https://doi.org/10.5194/acp-21-457-2021-supplement

Atmospheric Chemistry and Physics
Open Access
EGU

Supplement of

Global modeling of heterogeneous hydroxymethanesulfonate chemistry

Shaojie Song et al.

Correspondence to: Shaojie Song (songs@seas.harvard.edu)

- Text S1
- Figures S1–S11
- Table S1

Text S1. An example to explain the effect of Δt on the competition of reactions

Suppose there are two reactions that oxidize SO_2. The oxidants are assumed to be in large excess, and thus these two reactions are both first order with respect to SO_2. The initial concentration of SO_2 is C_0. The time step Δt is 20 min. One reaction is faster with a lifetime of SO_2 (τ_1) of 2 min. The other one is a factor of 100 slower, with a τ_2 of 200 min. Therefore, the first-order rate constants for these two reactions are $k_1=1/\tau_1=0.5$ min^{-1} and $k_2=1/\tau_2=0.005$ min^{-1}. The losses of SO_2 in this time step Δt can be calculated by Eq. 13 in the main text: $LS_1 = C_0\times[1-\exp(-k_1\times\Delta t)] \approx C_0$; $LS_2 = C_0\times[1-\exp(-k_2\times\Delta t)] = 0.095C_0$. Because the total losses cannot exceed C_0, we need adjust the individual loss by a factor of $C_0/(LS_1+ LS_2)$. The new LS_1 and LS_2 are $0.9C_0$ and $0.09C_0$, respectively. The calculations show, in this time step, that the losses of SO_2 due to these two reactions are different by a factor of 10, although their rate constants vary by a factor of 100. This example suggests an overestimation of the importance of the slower reaction while an underestimation of the importance of the faster one.

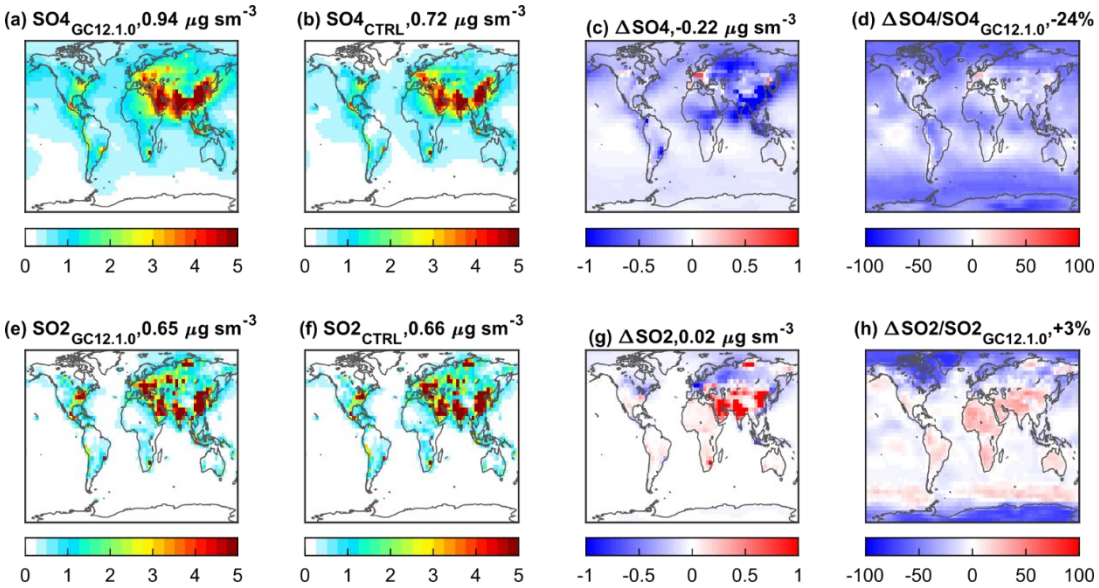

Figure S1. Surface concentrations of SO_4^{2-} (top) and SO_2 (bottom) from the standard GEOS-Chem v12.1.0 (GC12.1.0) simulation and from the control (CTRL) simulation. Values in panel titles are global averages. (c) is the absolute difference between these two simulations: b−a. (d) is their relative difference: (b/a−1)×100%. Similarly, (g) is the absolute difference between (e) and (f): f−e, and (h) the relative difference between them: (f/e−1)×100%. The concentration unit is μg sm^{-3}, where 1 sm^3 equals 1 m^3 at 273.15 K and 1013.25 hPa.

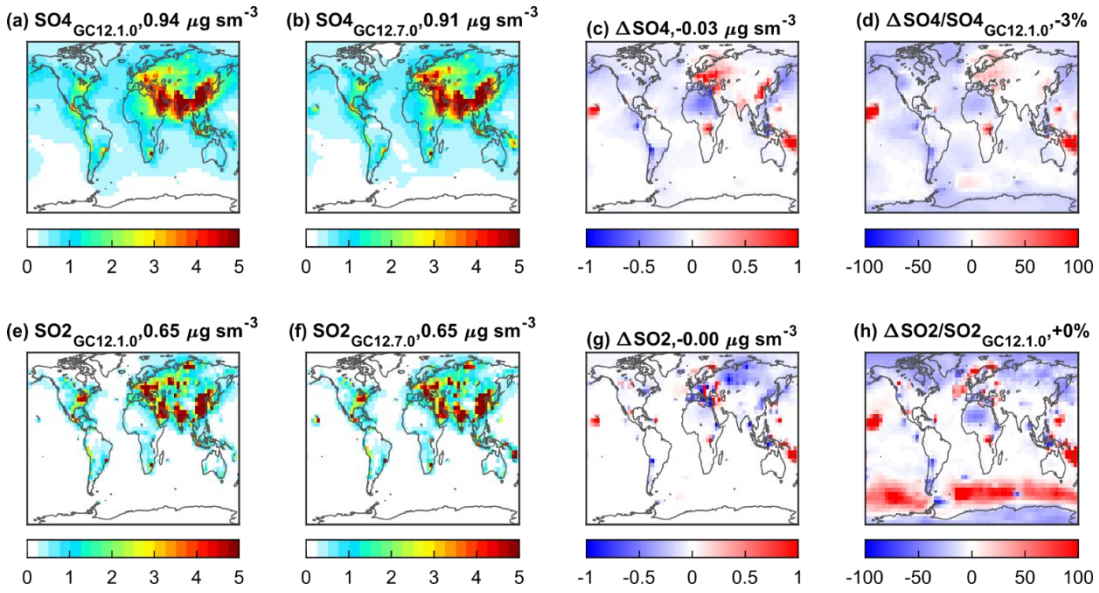

Figure S2. Surface concentrations of SO_4^{2-} (top) and SO_2 (bottom) from the standard GEOS-Chem v12.1.0 (GC12.1.0) simulation and from the standard GEOS-Chem v12.7.0 (GC12.7.0) simulation. Values in panel titles are global averages. (c) is the absolute difference between these two simulations: b−a. (d) is their relative difference: (b/a−1)×100%. Similarly, (g) is the absolute difference between (e) and (f): f−e, and (h) the relative difference between them: (f/e−1)×100%. The concentration unit is μg sm^{-3}, where 1 sm^3 equals 1 m^3 at 273.15 K and 1013.25 hPa.

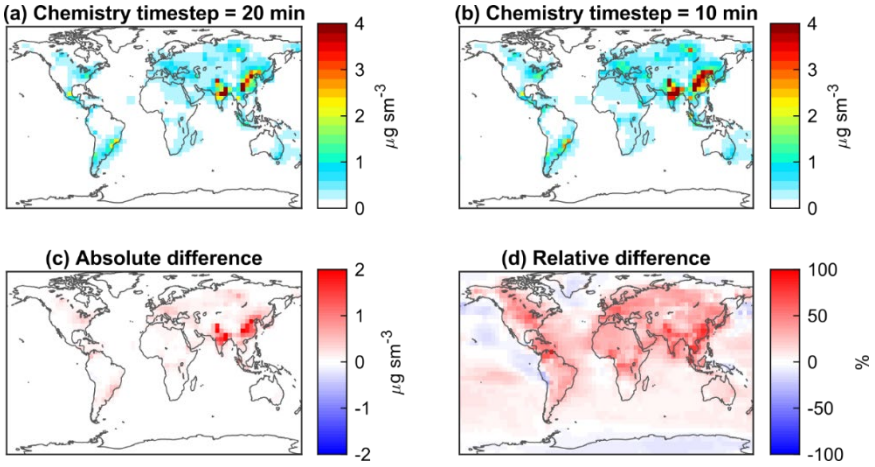

Figure S3. Surface SO_4^{2-} concentrations through the in-cloud O_3 chemical pathway in July. (a) shows the results from the control simulation. (b) shows the results from a sensitivity simulation in which the only difference from the control simulation is the chemistry time step is set to 10 min. (c) is the absolute difference between these two simulations: b−a. (d) is their relative difference: (b/a−1)×100%. The global mean concentration of SO_4^{2-} from (b) is higher by about 27% compared with that from (a). The concentration unit is μg sm^{-3}, where 1 sm^3 equals 1 m^3 at 273.15 K and 1013.25 hPa.

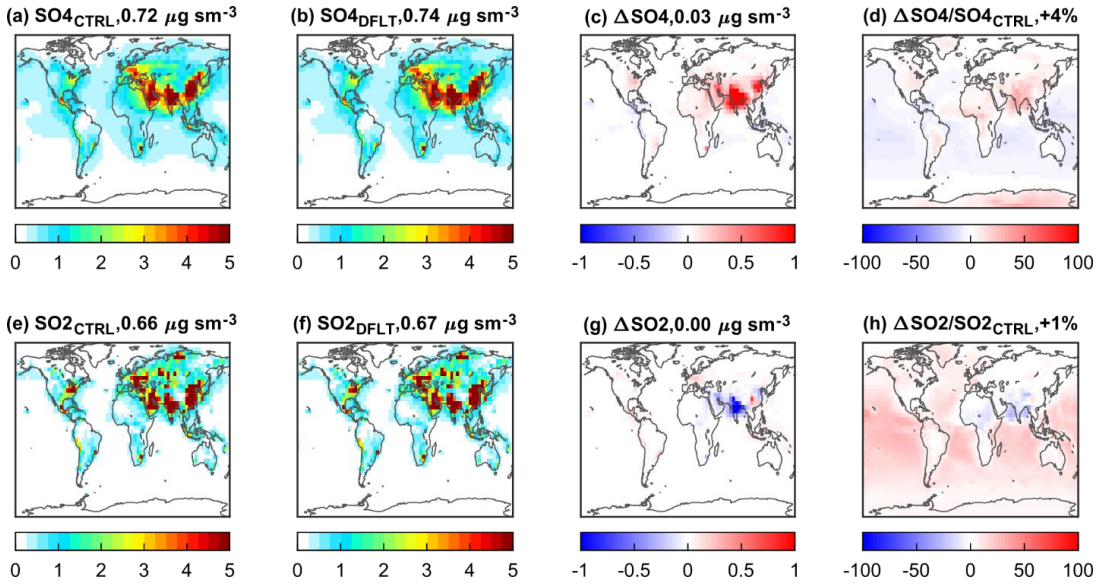

Figure S4. Surface concentrations of SO_4^{2-} (top) and SO_2 (bottom) from the control (CTRL) and default (DFLT) simulations. Values in panel titles are global averages. (c) is the absolute difference between these two simulations: b−a. (d) is their relative difference: (b/a−1)×100%. Similarly, (g) is the absolute difference between (e) and (f): f−e, and (h) the relative difference between them: (f/e−1)×100%. The concentration unit is μg sm^{-3}, where 1 sm^3 equals 1 m^3 at 273.15 K and 1013.25 hPa.

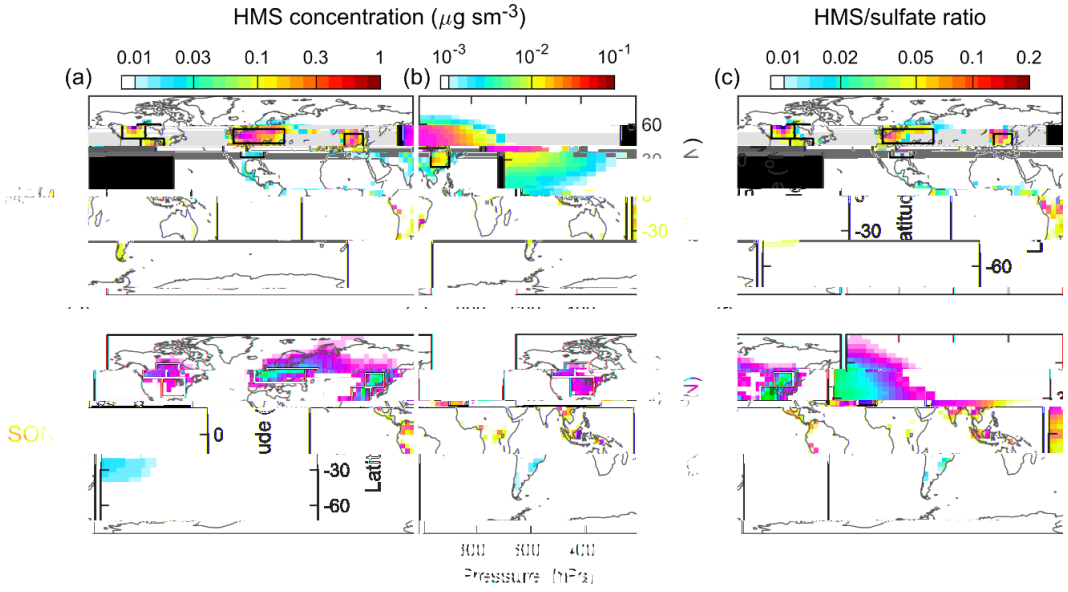

Figure S5. Distributions of the modeled HMS concentrations and the molar ratios of HMS to sulfate by the default simulation. Top and bottom panels show results for MAM (March–April–May) and SON (September–October–November), respectively. (a), (c), (d), and (f) are the horizontal distributions in the surface layer. (b) and (e) are the vertical distributions of the zonal averages from surface to 200 hPa. The concentration unit is μg sm^{-3}, where 1 sm^3 equals 1 m^3 at 273.15 K and 1013.25 hPa. The color bars are not linear and differ in the three columns. The same color bars are used for each pair of the top and bottom panels. The black-outline boxes indicate the three regions selected for quantitative analysis.

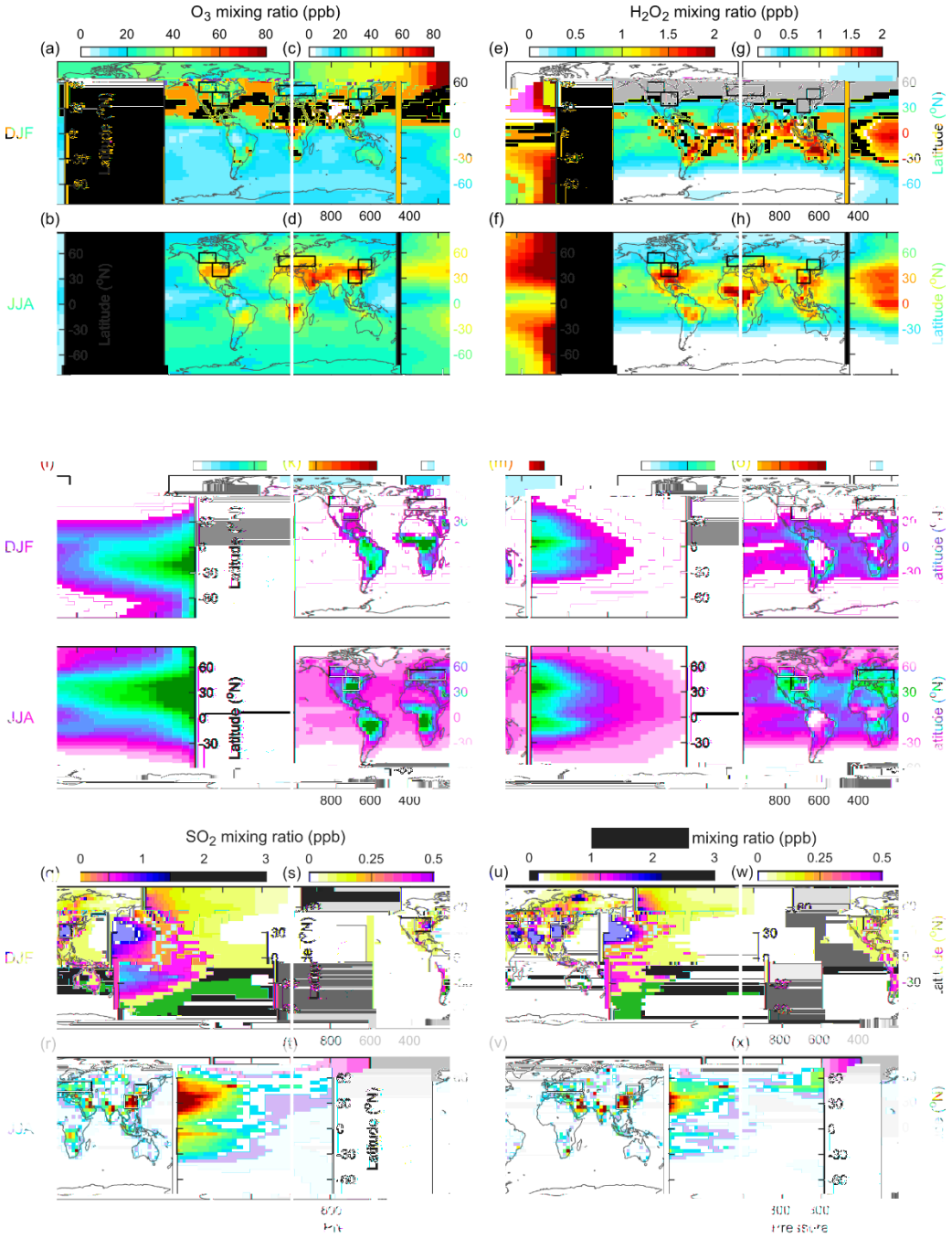

Figure S6. Distributions of the modeled mixing ratios of several species from the default simulation, including O_3 (a–d), H_2O_2 (e–h), HCHO (i–l), OH (m–p), SO_2 (q–t), and the geometric mean of HCHO and SO_2 ($\sqrt{SO_2 \times HCHO}$) (u–x). For each species, top and bottom panels show results for DJF (December–January–February) and JJA (June–July–August), respectively, and the left and right panels are, respectively, the horizontal distributions in the surface layer and the vertical distributions of the zonal averages from surface to 200 hPa. The same color bars are used for each pair of the top and bottom panels. All color bars are linear but may differ among species. The black-outline boxes indicate the three regions selected for quantitative analysis. The unit of these species is ppb expect for OH that is ppq.

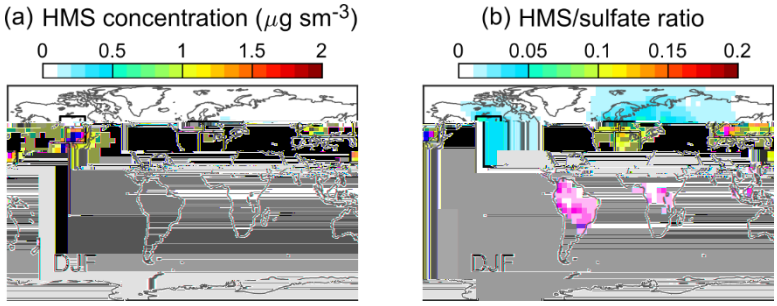

Figure S7. Surface HMS concentrations (a) and molar ratios of HMS to sulfate (b) in the default simulation for DJF (December–January–February). The color bars are linear. The concentration unit is μg sm^{-3}, where 1 sm^3 equals 1 m^3 at 273.15 K and 1013.25 hPa. The black-outline boxes indicate the three regions selected.

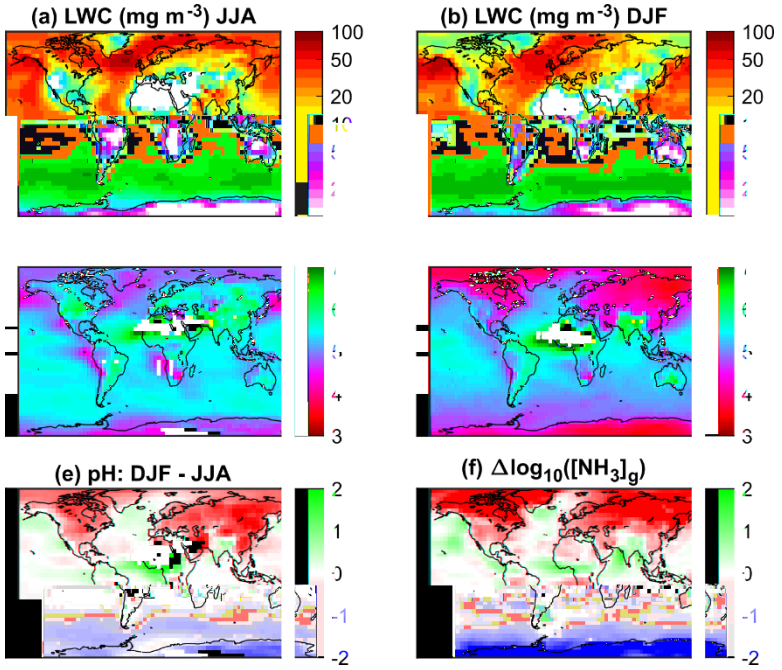

Figure S8. Horizontal distributions of cloud liquid water content (LWC) and cloud water pH in the lower troposphere modeled by the default simulation. LWC data are vertical-column-integrated for the 13 vertical layers above surface up to about 800 hPa. pH data are liquid-water-weighted and vertical-column-integrated. (a) and (b) show LWC results for DJF (December–January–February) and JJA (June–July–August), respectively. (c) and (d) show pH results for DJF and JJA, respectively. (e) is the absolute difference of pH between these two seasons: b−a. (f) shows the modeled difference in gaseous ammonia mixing ratios (on a logarithmic scale) between these two seasons (DJF−JJA), $\Delta \log_{10}([NH_3]_g)$. The gaseous ammonia data are air-volume-weighted and vertical-column-integrated for the lower tropospheric layers. The color scales differ by rows. The color bar for LWC is not linear.

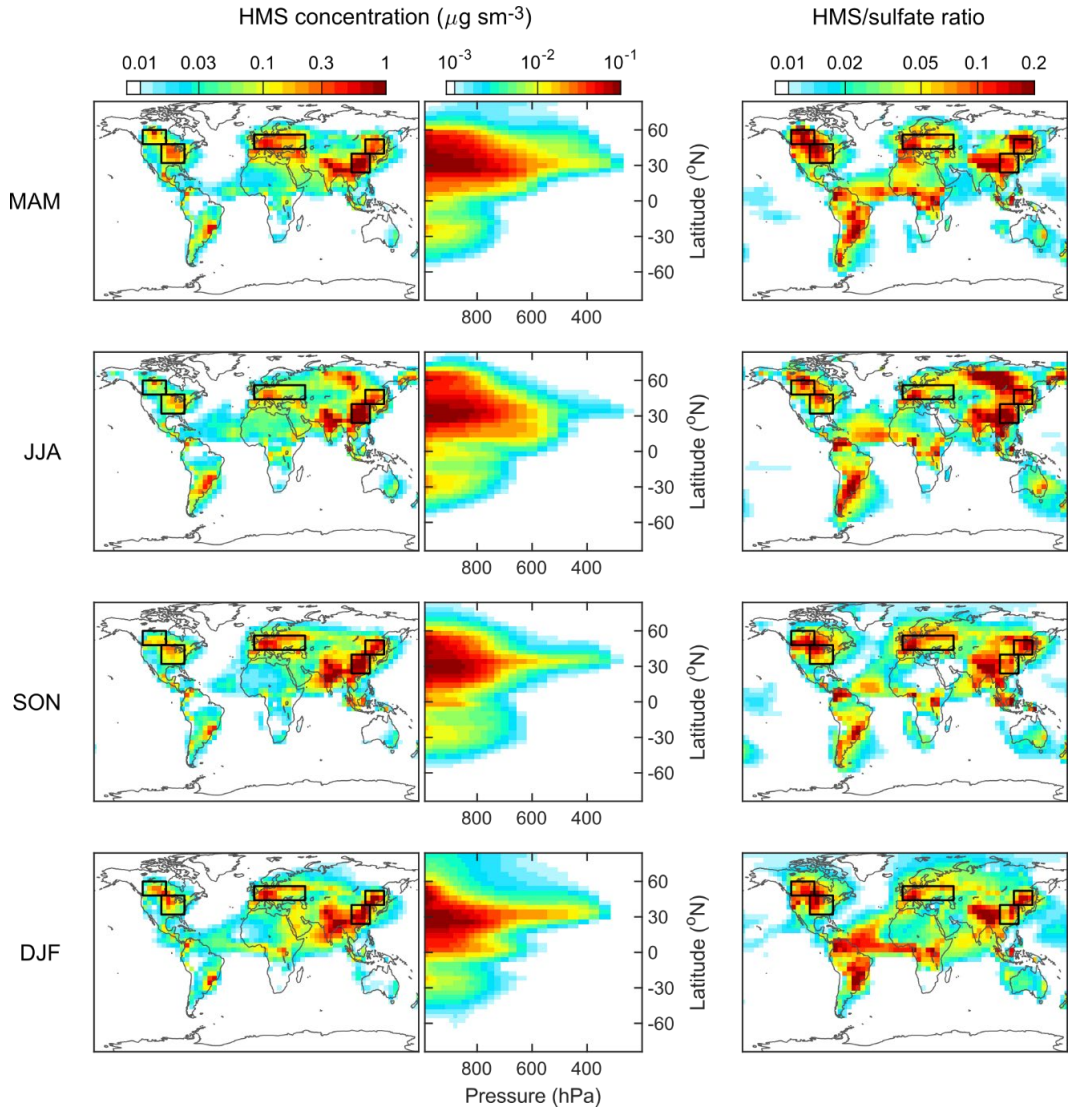

Figure S9. Distributions of the modeled HMS concentrations and the molar ratios of HMS to sulfate by the control simulation. The four rows are results for MAM (March–April–May), JJA (June–July–August), SON (September–October–November), and DJF (December–January–February), respectively. The first and third columns are the horizontal distributions in the surface layer. The middle column shows the vertical distributions of the zonal averages from surface to 200 hPa. The concentration unit is μg sm^{-3}, where 1 sm^3 equals 1 m^3 at 273.15 K and 1013.25 hPa. The color bars are not linear and differ in the three columns. The same color bars are used for each pair of the top and bottom panels. The black-outline boxes indicate the three regions selected for quantitative analysis.

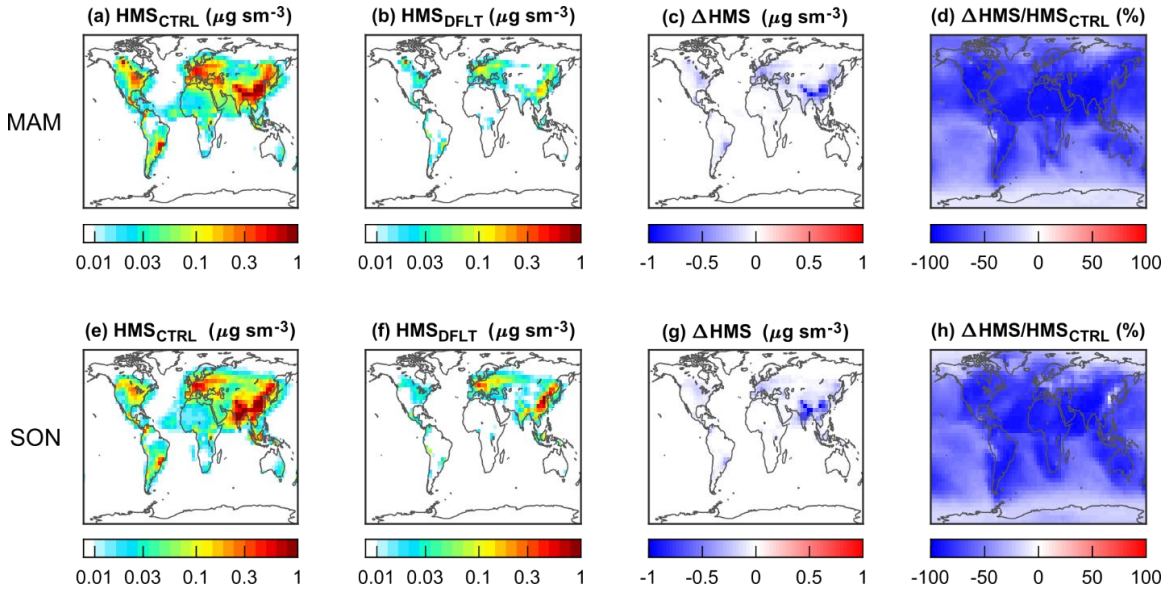

Figure S10. Surface concentrations of HMS from the control (CTRL) and default (DFLT) simulations in two seasons. Top and bottom panels show results for MAM (March–April–May) and SON (September–October–November), respectively. (c) is the absolute difference between these two simulations: b−a. (d) is their relative difference: (b/a−1)×100%. Similarly, (g) is the absolute difference between (e) and (f): f−e, and (h) the relative difference between them: (f/e−1)×100%. The concentration unit is μg sm^{-3}, where 1 sm^3 equals 1 m^3 at 273.15 K and 1013.25 hPa. The color bars in (a), (b), (e), and (f) are not linear.

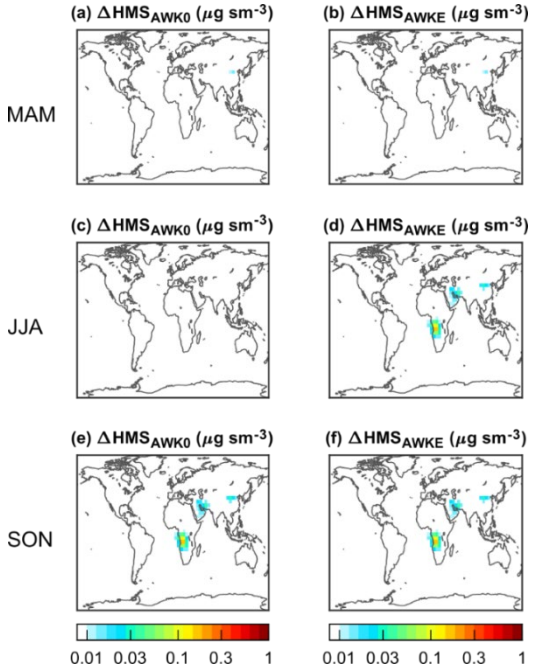

Figure S11. Difference in surface HMS concentrations between two sensitivity simulations (AWK0 (left) and AWKE (right)) and the default simulation (DFLT). The three rows are for MAM (March–April–May), JJA (June–July–August), and SON (September–October–November), respectively. The color bars are not linear.

Table S1. Statistics of the SO_2 lifetime (τ) for cloud reactions in two randomly selected weeks during summer and winter. The percentages in the table show the probabilities of $\tau < 20$ min and < 1 min. Data are calculated in the same way as Fig. 3 in the main text.

	July 3rd to 9th		January 3rd to 9th	
	$\tau < 20$ min	$\tau < 1$ min	$\tau < 20$ min	$\tau < 1$ min
Total of 7 reactions	56%	4.0%	29%	2.6%
$SO_2 + O_3$	41%	3.4%	19%	2.1%
$SO_2 + H_2O_2$	12%	0.0%	7.9%	0.0%
SO_2 + HCHO	1.4%	0.0%	1.0%	0.0%